Transport through an interacting system connected to leads

2003 J. Phys.: Condens. Matter 15 8805

(http://iopscience.iop.org/0953-8984/15/50/013)

INSTITUTE OF PHYSICS PUBLISHING JOURNAL OF PHYSICS: CONDENSED MATTER

J. Phys.: Condens. Matter **15** (2003) 8805–8826 PII: S0953-8984(03)64022-1

Transport through an interacting system connected to leads

G Chiappe[1] **and J A Vergés**[2]

[1] Departamento de Física J J Giambiagi, Facultad de Ciencias Exactas, Universidad de Buenos Aires, Ciudad Universitaria, 1428 Buenos Aires, Argentina
[2] Instituto de Ciencia de Materiales de Madrid, Consejo Superior de Investigaciones Científicas, Cantoblanco, E-28049 Madrid, Spain

E-mail: gchiappe@dfuba.df.uba.ar and jav@icmm.csic.es

Received 23 May 2003
Published 3 December 2003
Online at stacks.iop.org/JPhysCM/15/8805

Abstract

Keldysh formalism is used to find the current–voltage characteristics of a small system of interacting electrons described by a Hubbard model coupled to metallic wires. The numerical procedure is checked and the well known results for an Anderson impurity are found. When larger interacting regions are considered, quite different results are obtained depending on whether the Hubbard part is half-filled or not. At half-filling, the existence of an energy gap for charge excitations manifests itself by making the current exponentially small as a function both of the number of interacting sites and the value of U. The behaviour changes at large voltages above the gap energy when activated charge transport takes place. In contrast, for filling factors other than half, the current goes through the interacting system and suffers just a small amount of scattering at both connections. Conductance depends slightly on U and much more on the filling factor but not on the length of the interacting region.

1. Introduction

There are several reasons for studying the precise role played by electron–electron interactions in the transport of electric current through small systems connected to metallic electrodes. Among other things, we can look at quantum dot measurements in the Kondo regime, deviations of the exact conductance quantization in low-disorder quantum wires, the possibility of many-body effects in the transport through molecules, or we can even have quite fundamental discussions about the possibility of quantum dephasing at $T = 0$. However, in this paper we are not particularly concerned with the explanation of any detailed experimental results but with the methodological improvement of the numerical tools that can be used when studying many-body effects on the electric transport in small (either mesoscopic or nanoscopic) devices. For this purpose, we take the simplest interacting model (the one-dimensional Hubbard model)

connected to metallic leads and develop a precise numerical recipe to obtain results that make physical sense. The work by Maslov and Stone [1], Ponomarenko [2] and Schulz and Safi [3], showing that electrons can traverse a Luttinger liquid without suffering scattering, are direct precursors of our work. Of particular importance are the works by Oguri [4, 5] which studied the same model using exact second-order perturbation theory in the interaction and concluded that it is not only transport through a single interacting site that shows perfect transmission at half-filling (symmetric Anderson impurity) but also transport through *any* odd number of interacting sites. We will show that our results point to a regular odd–even behaviour leading to isolating transport characteristics well described by the existence of a finite energy gap for charge excitations. We will add physical arguments to our numerical results (see section 3.2). Additional theoretical contributions about transport through the 1D Hubbard model are collected in [6]. The theoretical method is presented in the next section while results are given in section 3. After checking the numerical method for only one interacting site (Anderson impurity), the conductivity of extended interacting systems has been studied both at and below half-filling. The last section summarizes our findings.

2. Theoretical method

The standard setup of transport measurements in mesoscopic systems is considered. Ideal metallic leads are connected to a central part containing the relevant part of the system: interacting electrons in our case. The evaluation of the current–voltage (IV) characteristic of the extended system proceeds in two steps. First, the central interacting part is exactly solved for a given number of electrons and a well-defined electrochemical potential profile by means of Lanczos-type techniques. Second, Keldysh formalism is used to attach *in an approximate but physically appealing way* the leads to the central region. Caroli *et al* [7] were probably among the first authors to use this kind of direct approach for the calculation of the tunnelling current through a non-interacting system. The extension of the formalism for the current through an interacting electron region was given by Meir and Wingreen [8]. The formalism depends crucially on the knowledge of the many-body self-energy describing interaction effects. Our numerical procedure gives a precise recipe for an approximate evaluation of this self-energy.

2.1. Finite system

The central region is described by a nearest-neighbours tight-binding Hamiltonian with on-site interaction terms among electrons of different spin. This is the well-known Hubbard model:

$$\hat{\mathcal{H}} = t \sum_{\langle i,j\rangle,\sigma} \hat{c}^{\dagger}_{i,\sigma}\hat{c}_{j,\sigma} + U \sum_{i} \hat{n}_{i,-\sigma}\hat{n}_{i,\sigma}, \tag{1}$$

where the label i denotes a generic site in the finite cluster, $\langle i, j\rangle$ represents nearest-neighbour pairs, and $\hat{n}_{i,\sigma} = \hat{c}^{\dagger}_{i,\sigma}\hat{c}_{i,\sigma}$ gives the number of electrons of spin σ at site i.

The presence of an external electrostatic potential is described by an additional one-electron term:

$$\hat{\mathcal{H}}_{\text{ext}} = -e \sum_{i,\sigma} \phi_i \hat{n}_{i,\sigma}, \tag{2}$$

being ϕ_i the value of electrostatic potential at site i. The Lanczos method allows the calculation of the ground state of the finite interacting system for a number of sites equal to or smaller than 14 at half-filling (computation is sometimes feasible for a larger number of sites when a smaller number of electrons is considered or system symmetries are explicitly used). Once the

ground state is known, a continued fraction expansion of the Green functions in a Lanczos-type basis allows their evaluation as a function of energy (see the review by Dagotto [9][3] for a detailed description). In fact, the four Green functions entering into the Keldysh formalism are explicitly calculated in this way [10–12]. A matrix form with site and Keldysh indices will be used for the whole set of Green functions of the finite cluster[4]:

$$\mathbf{g} = \begin{pmatrix} g^{--} & -g^{-+} \\ g^{+-} & -g^{++} \end{pmatrix}. \tag{3}$$

Notice that the ω-dependence of the Green functions is not shown in order to keep the notation clearer.

2.2. *Coupled system*

Green functions of the extended system (interacting central part plus electrodes) are obtained by means of a Dyson equation. Leads are described by a constant density of states equal to that at the band centre of a non-interacting chain with a hopping equal to t. For example, the Green function at the right end (site l) of the left electrode is:

$$t\mathbf{g}_{l,l} = \begin{pmatrix} \mathrm{i} & -2\mathrm{i} \\ 0 & -\mathrm{i} \end{pmatrix}, \tag{4}$$

for energies below the chemical potential μ_l of this electrode and:

$$t\mathbf{g}_{l,l} = \begin{pmatrix} -\mathrm{i} & 0 \\ -2\mathrm{i} & \mathrm{i} \end{pmatrix}, \tag{5}$$

for energies above μ_l. The Dyson equation is used to couple the central part to the leads *when* $U = 0$:

$$\mathbf{G_0} = \mathbf{g}(0) + \mathbf{g}(0)\mathbf{T}\mathbf{G_0}, \tag{6}$$

being the only non-zero elements of the hopping term $\mathbf{T}$ given by the following:

$$\mathrm{T}^{--}_{1,l} = \mathrm{T}^{--}_{l,1} = \mathrm{T}^{++}_{1,l} = \mathrm{T}^{++}_{l,1} = t_l, \tag{7}$$

which couples the first site 1 of the finite system to the left electrode and

$$\mathrm{T}^{--}_{L,r} = \mathrm{T}^{--}_{r,L} = \mathrm{T}^{++}_{L,r} = \mathrm{T}^{++}_{r,L} = t_r, \tag{8}$$

which couples the last site L of the central part to the right electrode. In this way, the non-interacting non-equilibrium Keldysh Green functions of the extended system $\mathbf{G_0}$ can be obtained from the $U = 0$ solution of the central part $\mathbf{g}(0)$. Many-body interactions are added to $\mathbf{G_0}$ by means of a second Dyson equation:

$$\mathbf{G} = \mathbf{G_0} + \mathbf{G_0}\boldsymbol{\Sigma}\mathbf{G}, \tag{9}$$

where $\boldsymbol{\Sigma}$ contains all contributions coming from the Hubbard interaction in (1). It is numerically obtained as the difference between the non-interacting Green function inverse and that including U effects:

$$\boldsymbol{\Sigma} = [\mathbf{g}(0)]^{-1} - [\mathbf{g}(U)]^{-1}. \tag{10}$$

This equation contains all the approximations needed to obtain the transport properties of the extended many-body system. They are:

[3] Non-diagonal elements of the Green function are obtained using linear combinations of fermion operators. For example:

$$\langle(\hat{c}_i + \hat{c}_j)^\dagger(\hat{c}_i + \hat{c}_j)\rangle = \langle\hat{c}_i^\dagger\hat{c}_i\rangle + \langle\hat{c}_i^\dagger\hat{c}_j\rangle + \langle\hat{c}_j^\dagger\hat{c}_i\rangle + \langle\hat{c}_j^\dagger\hat{c}_j\rangle.$$

[4] Although the notation of [11] is used in this paper, Green function matrices have been arranged according to the Mahan prescription (see [12]). This form allows non-diagonal self-energies having the same properties as the corresponding Green functions.

(i) Although $\mathbf{\Sigma}$ is spatially localized (remember that interaction is restricted to the central part), correlation among electrons visiting distant parts of electrodes is not taken into account.
(ii) The detailed form of the electrostatic potential inside the sample is not known.
(iii) Averages within the central part are evaluated using the equilibrium ground state of the cluster. They may be changed by the presence of an important potential bias inducing a large current through the sample.

Notice the quite different character of the three approximations we are using to find well-defined transport properties through the interacting system. The first one is just a computational limitation that can be eventually overcome with larger mainframes allowing the inclusion of parts of the electrodes until convergence of the self-energy can be reached. The second one is physically more relevant and has to do with Hartree consistency along the system. Although a charge-dependent term could be added to equation (1) and iteratively solved, we think that given the unrealistic one-dimensional nature of the model this could lead to numerical difficulties not directly related to physical properties. Therefore, we have preferred the inclusion of an arbitrary fixed form for the electrochemical potential inside the sample and just checked that our main results do not depend qualitatively on the selected profile. The third one is actually *the* approximation of this method. Naively, one could think that the many-body state of the interacting part when a current is flowing is not related to any state of the isolated system nor even to an easy combination of the ground state with some excited states. Since the self-energy defined by equation (10) directly depends on the state used to calculate Green functions, one should conclude that this is just an uncontrolled approximation that has to be validated *a posteriori* once results make sense.

Alternatively, many-body contributions to the self-energy can be calculated by perturbation theory. Typically, just the second-order diagram is considered [4, 13].

Simultaneous use of equations (6), (9), and (10) gives the main working equation of this paper:

$$\mathbf{G} = \mathbf{g}(U) + \mathbf{g}(U)\mathbf{T}\mathbf{G}, \tag{11}$$

where $\mathbf{G}$ is an approximate Keldysh Green function of the non-equilibrium many-body extended system. Equation (11) has been recently used for the study of Bohm–Aharonov and persistent currents through quantum dots in the Kondo regime and the transport in coupled quantum dots [14]. Seminal works using similar ideas to gather exact solutions of small many-body systems into a lattice are much older [15].

The explicit form of the global Keldysh Green function is:

$$\mathbf{G} = \begin{pmatrix} \mathrm{G}^{--} & -\mathrm{G}^{-+} \\ \mathrm{G}^{+-} & -\mathrm{G}^{++} \end{pmatrix}. \tag{12}$$

Any interesting physical magnitudes can be obtained from it. For example, the density of states at site i is:

$$N_i(\omega) = -\frac{1}{\pi}\,\mathrm{Im}(\mathrm{G}^{--}_{i,i} - \mathrm{G}^{-+}_{i,i}), \tag{13}$$

assuming spin degeneracy. If not the case, the spin label should be explicitly considered by doubling the size of the Green function matrices. Apart from this technical complication, the spin-dependent formalism remains exactly the same.

The occupied part is directly taken into account by the non-diagonal part of the Keldysh Green function formalism. Therefore, the charge on site i is given by:

$$q_i = \frac{e}{2\pi}\int_{-\infty}^{+\infty} \mathrm{d}\omega\ \mathrm{Im}(\mathrm{G}^{-+}_{i,i}). \tag{14}$$

In the same way, the current flowing from the left electrode to the first site in the central cluster labelled by 1 is:

$$I_{l,1} = \frac{et_l}{h} \int_{-\infty}^{+\infty} \mathrm{d}\omega \, (\mathrm{G}^{-+}_{1,l} - \mathrm{G}^{-+}_{l,1}). \tag{15}$$

Differential conductance is obtained as the derivative of the current versus voltage curve:

$$G = \frac{\mathrm{d}I}{\mathrm{d}V}, \tag{16}$$

and will be plotted as a function of the energy window eV opened by the source–drain voltage V. In the particular case in which voltage does not change the electrostatic potential inside the interacting region, G will coincide with the function inside integral (15). This magnitude gives (apart from a constant) the transmission as a function of band energy for a one-electron problem but differs from it in a general case due to the inclusion of inelastic effects. At zero bias, differential conductance and conductance are equal and can be straightforwardly compared with conductance values obtained within linear response theory:

$$G_{\mathrm{dc}} = t_l(\mathrm{G}^{-+}_{1,l}(\mu) - \mathrm{G}^{-+}_{l,1}(\mu)), \tag{17}$$

where Green functions are evaluated at the equilibrium chemical potential energy μ.

3. Results

The numerical method described in the previous section is still not fully determined. Before giving the results that we believe better describe the physical problem, we have to give the details that allow the calculation of a unique current–voltage (I–V) characteristic for the problem.

The first issue is the value of the electrostatic potential entering into the central part [16]. Ideally, one could use the Poisson equation to obtain the potential from a knowledge of the charge distribution. This would imply a self-consistent calculation involving the whole system formed by electrodes and the interacting part. As said before, the one-dimensional character of the problem adds both technical and physical complications to the problem. As a consequence, we have preferred the use of a model potential profile that is numerically convenient and does not bias the results. Two choices have been tried, either a constant potential inside the central part (that implies potential discontinuities at the boundaries) or a linear form matching the value of the potential at the electrodes. The first one seems more appropriate for a metallic situation in which the electric field inside the sample vanishes whereas the second choice could describe an isolating behaviour that allows the formation of a large electric field inside the central part. Notice that both choices imply the accumulation of charge at the electrode boundaries. Results for the first choice will be presented in the paper although checks have systematically been run to assure that conclusions are model-independent.

The second issue has to do with the correct description of the interfaces between electrodes and sample. Since our main approximation to the many-body nature of the problem comes from the use of a self-energy obtained for a finite system, the inclusion of one or more non-interacting sites within this finite part seems appropriate. Unfortunately, the correct description of a wide band metal requires more than one orbital per site and a precise model for the one-electron hopping elements. Note that the use of a Hamiltonian like (1) with $U = 0$ for the electrodes could produce important deviations from the correct results. For example, when electrons traverse the interacting part through the upper Hubbard band at energies around U, the electrode should have a finite density of states at this energy to allow electronic transport. This is not the case for the chain model with a band between $-2t$ and $+2t$ when U is large enough ($U > 2t$ suffices). The same happens at half-filling when a Kondo-like resonance allows good

electronic transmission at $U/2$. In this work, in which methodology takes precedence over the real world, we will use electrodes described by a single band of width $4t$ *but* conveniently shifted to allow the electronic current coming from the interacting part[5]. Therefore, when some part of the electrodes is included in the heavy part of the calculation, atomic levels will be zero when transport is through the lower Hubbard band, U when transport is through the upper Hubbard band, and $U/2$ at half-filling when resonances within the gap could eventually allow charge transit. Non-interacting sites included in the Lanczos part of the calculation will be referred to as the interface region or salvage sites in the rest of the paper.

Now, we are prepared to list the numerical steps that are followed to get the current–voltage characteristic of an arbitrary system. First, the ground state for a given cluster occupation is obtained and, second, the tridiagonal form of all needed Green functions is evaluated. Third, the chemical potential of the finite cluster is obtained from two additional ground state Lanczos calculations for one more and one less particle (the arithmetic mean is actually used). Fourth, the external voltage difference V is divided into equal parts that are added (subtracted) to the chemical potential (the one obtained in the previous step) of the left (right) electrodes. Fifth, equation (11) is used to obtain the Keldysh Green function that provides the non-equilibrium description of the coupled system. With these ingredients, application of equation (15) allows the calculation of the current–voltage characteristic of the whole system.

Although straightforward and non-biased, the sketched numerical recipe implies non-checked approximations. The results presented in sections 3.2 and 3.3 provide some credibility to the method because they are physically meaningful and consistent. Nevertheless, we have conducted a more specific test for just a one site system: the one-dimensional Anderson impurity problem.

3.1. Anderson impurity

In this problem only electrons at one particular site labelled 0 suffer an interaction via a Hubbard term. Both the one-electron energy of this particular level and its hopping to nearest-neighbours are usually different from those for the rest:

$$\hat{\mathcal{H}}_{\mathrm{imp}} = \sum_{\langle i,j\rangle,\sigma} t_{ij}\hat{c}^{\dagger}_{i,\sigma}\hat{c}_{j,\sigma} + \epsilon_0 \sum_{\sigma} \hat{n}_{0,\sigma} + U\hat{n}_{0,-\sigma}\hat{n}_{0,\sigma}\,, \tag{18}$$

where $t_{ij} = t$ everywhere except at the impurity site. In effect, $t_{01} = t_{10} = t_{0\bar{1}} = t_{\bar{1}0} = 0.3t$ have been taken as representative of a weakly connected dot with more or less relevant many-body interactions given by U.

Notice that Hamiltonian (18) describes an infinite chain while Hamiltonian (1) in section 2.1 refers to a finite cluster. Our theoretical method is easily adapted to this problem considering the interacting site plus some additional sites at each side as the finite system while the remaining semi-infinite chains are now the electrodes.

Firstly, the system has been studied at half-filling, i.e. when just one electron occupies the central site. This happens when the impurity level ϵ_0 lies at $-U/2$. One or more salvage sites have been added to each impurity site to allow the coupling of the spin at the impurity with the spin of the conduction band electrons. An odd number of non-interacting sites should be added to each impurity site to allow the coupling between band states at its centre and the impurity level at the same energy. Since the hopping between impurity and lateral chains is usually much smaller than t, an even number of salvage sites giving states in $\pm\epsilon$ pairs do not

[5] Notice that a detailed description of levels and hoppings is only necessary for the sites coming into the numerical finite cluster calculation. The far part of the electrodes is still described by a constant density of states through the local Green functions given in (4) and (5) for the left electrode and similarly for the right one.

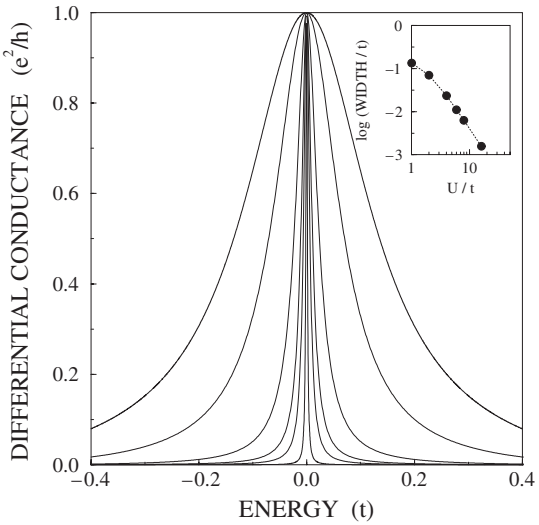

Figure 1. Differential conductance per spin channel through a single Anderson impurity in a half-filled situation plotted as a function of the energy window eV for several U values ($U/t = 1, 2, 4, 6, 8, 16$). The inset shows the resonance width as a function of U/t in a log–log representation.

couple appreciably to the impurity and are useless for our purpose. In this way, we typically end up with a system formed by an odd number of sites with an odd number of electrons. The corresponding ground state is a doublet. We take care of the spin degeneracy of the ground state including a spin index in all Green function matrices that consequently double their dimensions. In doing so, the final results do not depend on the particular linear combination chosen as the ground state.

It is well-known that a sharp resonance develops at the Fermi energy giving rise to perfect transmission through the one site cluster (Kondo resonant tunnelling [17]). Figure 1 shows this resonance and how it becomes narrower as the interaction U increases. Although differential conductance has been plotted as a function of the conducting energy window eV, results for the spectral weight on the impurity site are very similar. The results shown in the figure have been obtained for a finite cluster formed by 11 sites with the impurity at its centre after connecting the electrodes. While the U dependence of the resonance width follows the correct trend, an exponential narrowing of the resonance is not obtained. Actually, the width of the resonance follows a U^{-2} law that is shown in the inset of the figure.

Secondly, the system has been displaced from half-filling by varying the impurity level. The number of electrons in the cluster is fixed by the chemical potential of the metallic band. Typically, we have one electron on every system site except at the impurity where the occupation per spin varies from 0 to 1 as its level moves from $+\infty$ to $-\infty$. Transmission at the Fermi level is close to 1 when occupation is close to 0.5 and decreases rapidly when the number of electrons on the impurity site changes. The precise relationship between charge and conductance is determined by the Friedel–Langreth sum rule (see, for example, equation (7) of [17] and [18]). When the impurity is symmetrically coupled to both semi-infinite chains, the relation is given by:

$$G_\sigma = \sin^2(\pi \langle n_{0,\sigma} \rangle). \tag{19}$$

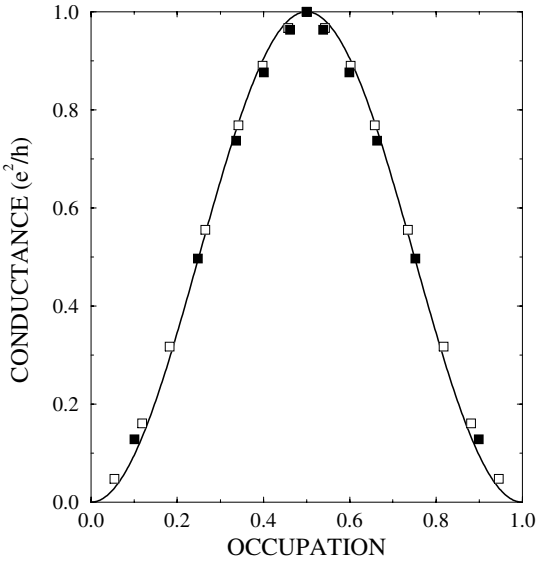

Figure 2. Relation between the conductance through a single Anderson impurity and its charge. Numerical results corresponding to $U = 4t$ and several values of the impurity level from $-5t$ to t are given by squares (open for a central cluster made by seven sites and filled for the larger cluster formed by 11 sites) and compared with the exact result based on the Friedel–Langreth sum rule (continuous curve).

Figure 2 gives the results for clusters formed by seven and 11 sites connected to half-filled electrodes. Here, the value of U is always $4t$ while the impurity level takes values between $-5t$ and t. It can be seen that the fulfilment of the exact relation is excellent regardless of the number of sites used to obtain the many-body self-energy[6].

We conclude that the Anderson impurity is well described by our numerical procedure even though a naive estimation of the extension of correlations suggests many more sites than included in the exact cluster calculation. Notice that although correlation self-energy is local, it produces long distance effects well within the semi-infinite chains. Pictorially, one can say that any state coming from one electrode suffers scattering by the many-body self-energy at the impurity site when travelling to the other electrode. In our scheme, correlation effects among these extended states just come from the components that they have on the finite cluster states that are exactly described by the Lanczos computation.

3.2. Half-filled system

Half-filling of the Hubbard model happens when the number of electrons equals the number of sites. The half-filled Hubbard model is an isolator because charge excitations occur through an energy gap which is of the order of U for large interaction values [19, 20][7]. This exact

[6] When calculating the many-body self-energy, the number of electrons present in the small cluster equals the number of sites. When the extended system is solved, a new Fermi level is defined at the energy at which the number of electrons in the cluster remains unchanged. The shift of the effective Fermi level diminishes for larger clusters and would eventually be zero for large enough systems. This procedure is consistent with the idea that electrons flowing into or out of the impurity come from very large distances.

[7] Numerical calculations of the optical conductivity of the Hubbard model in a ring geometry show an exponential decay of the Drude weight as a function of the number of sites. This scaling indicates an undoubtedly isolating behaviour of large samples.

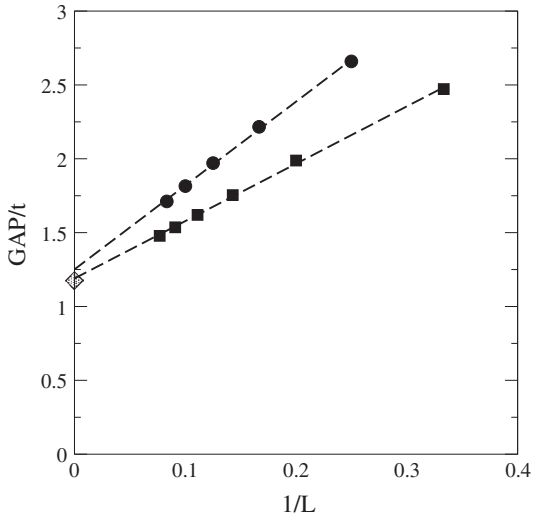

Figure 3. Size dependence of the gap of the Hubbard model at half-filling for $U = 4t$. Circles (squares) give results for even (odd) numbers of site values L while the diamond gives the exact value of Lieb and Wu [19] corresponding to infinite L. The straight dashed lines have been obtained by linear regression to the numerical data.

result proved by Lieb and Wu [19] using the Bethe ansatz is easily recovered by a finite cluster calculation both for even and odd numbers of sites (and a corresponding equal number of electrons) in spite of the apparent difficulty in dealing with an odd number of electrons in half the cases. When the number of sites is odd, either an up spin electron or a down spin electron is unpaired but for any choice the total density of states shows a gap. Partial up spin and down spin densities of states are different but share the same gap feature. Integration of these densities of states up to the gap gives the number of up and down spin electrons really present in the system. Figure 12 later in this paper shows an example density of states for 11 interacting sites while figure 3 shows how the gap scaling towards the exact Lieb and Wu result proceeds. Results for clusters formed by an even or odd number of sites and electrons scale along different straight lines that converge to the same limit. The gap is systematically smaller for the spin degenerate case. If one finds a spin polarized ground state (and consequently, a spin polarized density of states) uncomfortable, a mixed ground state can be formed as a linear combination of $S_z = \frac{1}{2}$ and of $S_z = -\frac{1}{2}$ states and spin polarization disappears when the weights of both components are equal. The gap in the density of states does not change. This behaviour has a very simple physical explanation that has very important consequences for transport properties. No matter what the spin of electrons, the energy cost for one less or one more electron within the system is about U at half-filling because every site is occupied by just one electron. Transport of electrons through the system implies a change of 1 in the number of electrons of the system and consequently an energy cost of the order of U. Electrons having just a bit more energy than the chemical potential in a dc experiment are unable to traverse the cluster. More precisely, the Green function of the coupled system develops exponential tails within the Hubbard cluster and conductance should scale towards zero for large enough systems. Our results below give a detailed description of this situation.

The previous paragraph has shown that odd clusters have nothing special in spite of spin degeneracy. Therefore, it is quite surprising that Oguri [4, 5] claims perfect transmission through interacting clusters formed by an odd number of sites larger than one based—at least

partially—in spin degeneracy. Notice that the only way of getting perfect transmission is the presence of a state (or resonance) at the chemical potential, i.e. at the gap centre in the symmetric case. While this state is absent in an exact cluster calculation, it is present in Oguri's Green functions because an odd number of one-electron states implies a state at the band centre and the exact but just second-order perturbation theory in the electron repulsion U that he performs is unable to open a gap. This was precisely the reason given by Oguri for his result in the first paper of the series[8]. What then is the physical reason for perfect transmission across *one* interacting site (Anderson resonance) but not for three or more interacting sites? Although not a mathematical argument, there is a simple reason for this behaviour: states in the whole system can be classified as even or odd according to their reflection symmetry relative to the central atom of the interacting region. When this region is formed by a single atom *but only* in this particular case, odd states do not couple to the interaction. Then a Fermi picture for the whole interacting ground state is possible in which some of the occupied states are purely one-electron states. If the last occupied state corresponds to one of these states, perfect transmission appears. This is always the case for an extended system but just happens in our finite cluster calculations when the number of odd states is odd and one of these purely one-electron states defines the Fermi level. This means 1 + 1 + 1 (the first integer gives the number of sites at the left side of the interacting region, the second one is the number of interacting sites and, the last integer the number of sites at the right side of the interacting region), 3 + 1 + 3, . . . systems but not 2 + 1 + 2, 4 + 1 + 4, as we have seen in section 3.1. As a direct consequence of this naive picture of the real complex many-body ground state, it is clear that the number of electrons that occupy the non-interacting state at the chemical potential can be 0, 1 or 2 without energy change. We have checked that this is indeed the case for the clusters used in 3.1 (the actual multiplicity of the cluster ground state is four: one spin doublet for which the number of electrons and sites coincide, a spin singlet with one extra electron and a second spin singlet with one less electron). This situation directly leads to a Green function showing zero energy *charge* excitation which explains the appearance of perfect transmission. Summarizing our point of view, there is a nice physical reason for perfect transmission across one interacting site but the persistence of perfect transmission across large interacting regions contradicts the insulating character proved for the Hubbard model by Lieb and Wu [19].

Let us come back to a detailed numerical study of transport through half-filled systems once the overall incorrectness of the Oguri results has been shown. Based on the familiar results of a standard one-electron isolating material, one can naively think that current–voltage characteristics will show an activated behaviour for voltage values above the charge excitations gap. In fact, this is the result if the self-energy corresponding to a pure finite Hubbard chain is used in the transport equation (15). This should be so since the many-body self-energy entering into the global Green function describes the charge gap. This behaviour does not change if one or more salvage sites are added to each side of the cluster that is numerically solved. Nevertheless, scaling proceeds differently for clusters formed by an even number of sites (and electrons) for which the ground state is a singlet and clusters of odd numbers of sites (and electrons) for which the ground state is a doublet. In the last case, we can speak of Kondo-like systems that show a tendency to form resonances with good transmission properties at the chemical potential energy $U/2$. Just to give a first example, figure 4 shows the qualitative change in the transport properties of Kondo-like clusters when interface sites are or are not included in the self-energy calculation: while the conductance of the system that completely ignores the electrodes has a minimum at the chemical potential due to the formation of a

[8] Notice that recovering the incorrect Oguri's result within our more general scheme is straightforward: it involves the use of the second-order self-energy of the cluster instead of the exact one that we use.

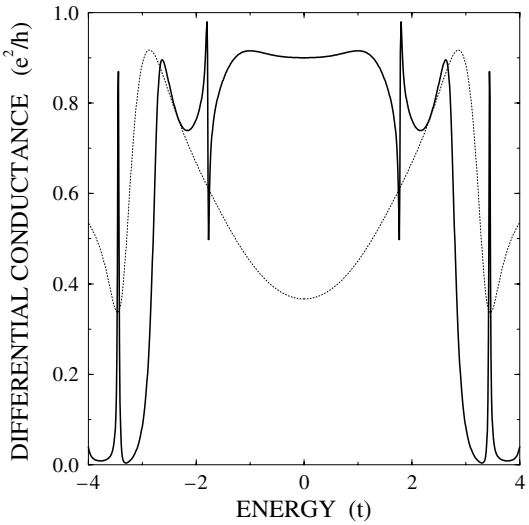

Figure 4. Transport through three interacting sites directly coupled to the electrodes (dotted curve) or coupled to the electrodes through one salvage site at each side (thick continuous curve). Results are given for $U = \pi t$.

pseudo-gap, transmission is almost maximum over a large energy range when one electrode site is included at each side. Physically, this result can be interpreted by saying that the unpaired electron of the small cluster forms a singlet with the band state at the chemical potential *only* if some electrode sites are included in the calculation of the correlation self-energy. We will begin showing the behaviour of the simpler systems (even number of sites) and come back to the degenerate case (odd number of sites) at the end of the section.

Size scaling of the problem at hand is shown in figure 5. Current–voltage curves have been obtained for Hubbard chains of increasing length (from two to 12 sites) and interaction $U = 4t$. The number of electrons in the chain equals the number of sites. The chemical potential is exactly $U/2$ in this situation. Figure 5 shows an exponential decrease of the current as a function of the length of the interacting part:

$$I \propto \exp(-\alpha L),$$

which implies

$$\log(I) \propto -\alpha L.$$

The linear L dependence in the logarithmic scale can be observed for any value of the potential below the gap (which is about $1.75t$ for $U = 4t$). This exponential scaling law is valid for any value of U. Consequently, a large enough interacting region completely prohibits current below the gap energy at half-filling.

Figure 6 shows the U dependence of a system formed by 12 sites. From top to bottom the IV curves for U/t values from 1 to 8 (in steps of one unity) have been plotted. It can be seen that the U dependence is quite similar to the previously seen L dependence. As before, current exponentially vanishes as a function of U (for U values larger than $3t$ at this size) for any potential value below the charge gap. The same data have been plotted in figure 7 in a linear–linear scale to emphasize the behaviour of the current for energies above the gap. It can be seen that an almost linear increase of almost maximum conductance slope takes place regardless the value of U. That means that electrons can enter the interacting system at

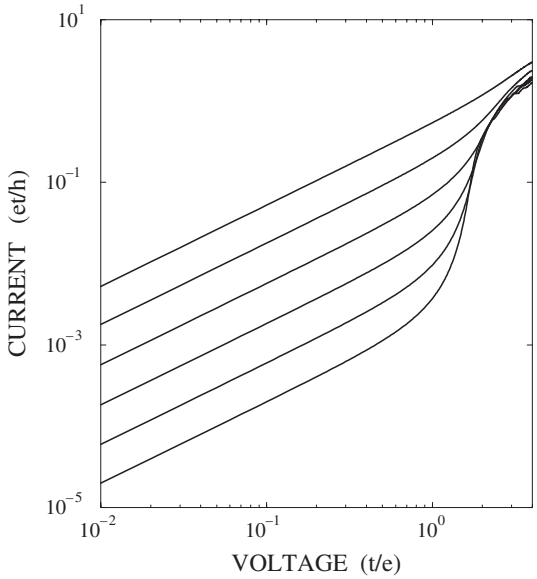

Figure 5. This figure illustrates the size scaling of our results at half-filling for an arbitrary value of the interaction $U = 4t$. Curves correspond to system lengths L from 2 (top) to 12 (bottom) in steps of two sites. The exponential dependence on chain length is manifested by the parallelism of the current–voltage curves at voltages below the charge gap. The same trend is followed at other U values although the exponential scaling of the current begins at larger lengths for smaller interactions.

energies in the lower Hubbard band and exit at energies corresponding to the upper Hubbard band, suffering just a small amount of scattering. We will discuss this apparent absence of scattering once the results at fillings different from half (metallic situation) are given.

Let us perform a detailed comparison with Oguri's results for the electronic transport through three and four interacting sites connected to reservoirs [5]. Our results are shown in figure 8 and should be compared with panel (a) (corresponding to zero temperature) of figures 10 and 11 of the mentioned paper[9]. While transmission across the three-site system are comparable, in particular for energies within the non-interacting band, results for the four-site system have nothing in common. Our results show the appearance of a pseudo-gap for the smaller U value and a well-developed gap for $U = 2\pi t$ (larger than the one-electron bandwidth) while Oguri's results for this size are similar to the ones for the smaller system. This result is a direct manifestation of the impossibility of forming a gap using the perturbative method of [5]. A closer look at the three-site system shows that our calculated transmission at the band centre is not 1 (as has been discussed before) although values close to 1 are reached at other energies.

The size dependence followed by spin-degenerate clusters is exemplified in figure 9. From top to bottom the size of the interacting part increases from one site to seven sites. It is evident that transmission rapidly diminishes with system size: in effect, the result at the bottom shows

[9] Strictly speaking, the differential conductance obtained by our approach and the many-body transmission probability given by Oguri in [5] have different physical magnitudes. Nevertheless, we believe that in the absence of a source–drain voltage dependence of the ground state of the finite cluster, our energy-dependent G is basically scanning the transmission of the states within the allowed energy window. In particular, both magnitudes converge to 1 for all states within the non-interacting band when U vanishes.

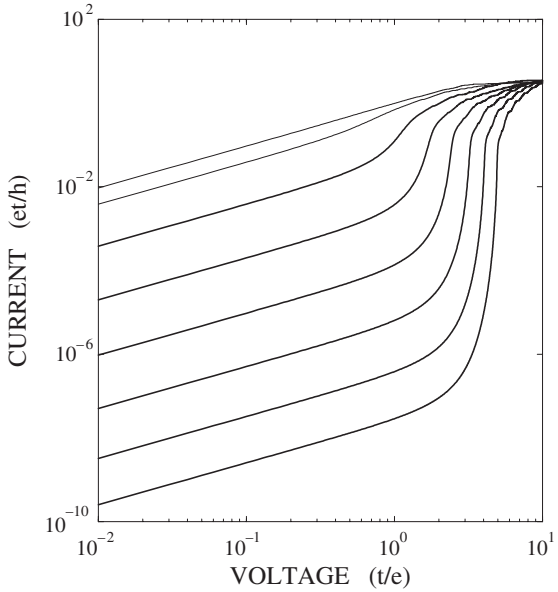

Figure 6. This figure illustrates the U dependence of the current–voltage curves at half-filling for a system of fixed size (12 sites). U goes from t (upper curve) to $8t$ (lower curve) in t steps. As in the previous figure, the exponential dependence is manifested by the parallelism of current–voltage curves at voltages below the charge gap. This happens for a U value larger than $3t$ for this system size. The systematic gap enlargement due to the increasing value of U is also shown by the figure.

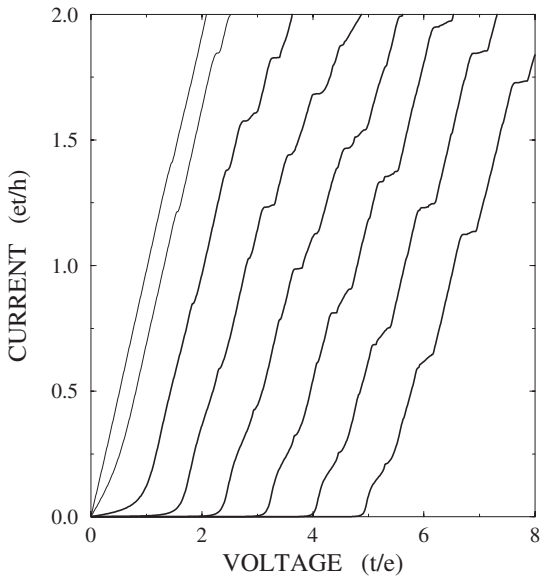

Figure 7. This figure illustrates the U dependence of the gap at half-filling for a system of fixed size (12 sites). The data of previous figure are plotted here in linear–linear scale: U increases from t to $8t$ in t steps for curves from left to right. Current–voltage characteristics show here in a clearer fashion the activated behaviour of current for voltage values above the gap charge.

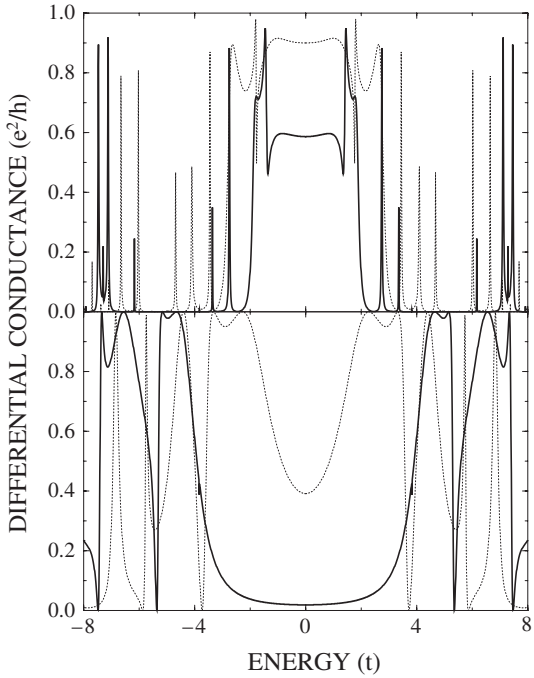

Figure 8. Differential conductance of small clusters for $U = \pi t$ (thin dotted curves) and $U = 2\pi t$ (thick continuous curves). Upper panel: three interacting sites embedded in a five-site cluster. Lower panel: four interacting sites.

narrow resonances in a developing gap (dashed curve gives the result excluding electrode sites, i.e. avoiding the formation of singlet cluster-band states). Figure 10 shows the dependence on the number of salvage sites included in the Lanczos finite cluster calculation. Conductance at zero bias is given for two, three, five, and seven interacting sites for cluster sizes of up to 14 sites. While the addition of salvage sites somewhat diminishes the conductance through two interacting sites, it increases the conductance of systems formed by an odd number of sites. Numerical data have been fitted by parabolas both for simplicity and because an L^{-1} fit has been quite successful in describing the gap formation (see figure 3). Although an extrapolated value of 1 cannot be excluded for the three-site result, it seems quite unlikely that the data for five and seven sites (two lower parabolas) extrapolate to 1.

In conclusion, our results show that when size scaling is correctly taken into account, all systems converge to the same physical behaviour at half-filling: current diminishes exponentially at voltages below the charge excitation gap due to the existence of this gap. Larger U values accelerate the scaling. At the end, no odd–even differences survive. Nevertheless, it is clear that the correct treatment/scaling of Kondo-like systems (formed by any odd number of impurities) requires much more care since results for small systems strongly depend on the details (presence or not of salvage sites, the precise description of these *metallic* sites, the number of them, etc).

At this point, a comparison of our results with recently published work studying persistent currents in rings [21, 22] is in order. In these works an interacting model of spinless fermions is studied instead of the Hubbard model to keep computational needs at a minimum level and make possible a clear extrapolation to the case of an infinitely large non-interacting part.

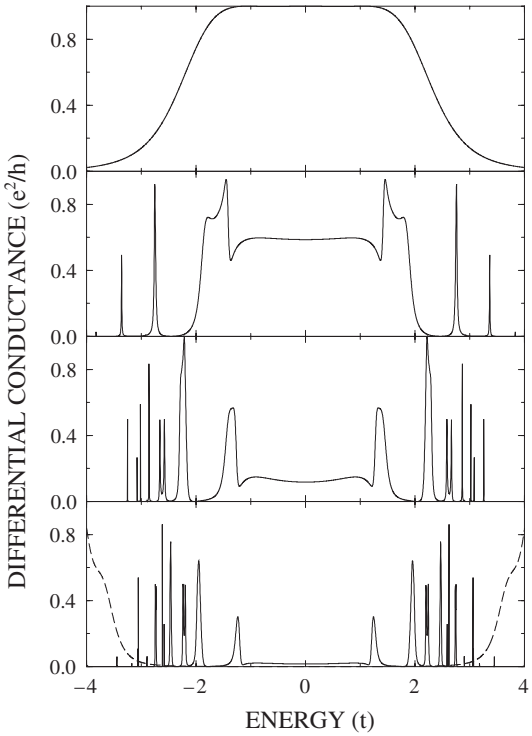

Figure 9. Differential conductance of clusters formed by an odd number of sites for $U = 2\pi t$. From top to bottom: one, three, five, and seven interacting sites plus one salvage site at each cluster side. The dashed curve in the bottom panel gives the differential conductance of a seven-site cluster with no salvage sites: the presence of a gap is evident.

Based on a result that has been proved for non-interacting systems, the conductance through a finite interacting region can be obtained from the comparison of the ring currents before and after switching on the interaction. Here, we will compare the conductances presented in figure 2 of [21] and figure 3 of [22] with the results obtained in our scheme when the Hubbard interaction between electrons of opposite spins at the same site is substituted by the following model of spinless fermions interacting with particles at nearest-neighbour sites:

$$U \sum_{i=1}^{L_s-1} (\hat{n}_i - 1/2)(\hat{n}_{i+1} - 1/2). \tag{20}$$

Let us begin discussing the more conventional case of an even number of sites L_s occupied by $L_s/2$ fermions. We take $L_s = 6$ (fermions on these sites interact with other fermions at nearest-neighbour sites) and add from one to eight salvage sites at each side of the interacting part (fermions just hop over these sites but no additional interaction exists). First, exact Green functions are calculated for this finite cluster following our standard procedure and then equation (11) is used to find approximate Green functions of the infinite connected system. Linear response conductances are obtained from non-diagonal Keldysh Green functions at the chemical potential which is zero at half-filling (see equation (17)). Figure 11 shows our results for U values 2 (circles) and 4 (squares) together with polynomial extrapolations to the limit of a large number of salvage sites. Conductance strongly depends on the even–odd character of the number of extra sites added to each side of the chain. Therefore, regression should take

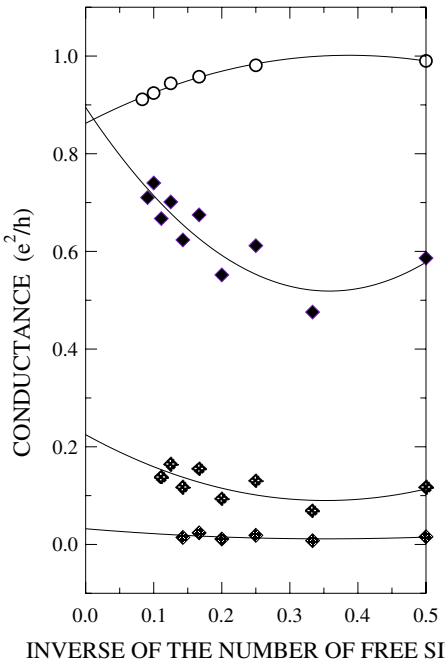

Figure 10. Dependence of the conductance at zero bias on the number of salvage sites included in the Lanczos finite cluster calculation. Circles and diamonds of decreasing density give results for two, three, five, and seven interacting sites when $U = 2\pi t$. Continuous curves give parabolic extrapolations to the infinite limit. Configurations with an even number of sites at both sides have not been considered as they artificially drop conductance. For example, eight salvage sites are asymmetrically distributed: three at one side and five at the other.

care of this particularity but converges to a more or less well-defined value. Our extrapolated conductances nicely agree with the values obtained for rings for both U values. Actually, the oscillatory convergence of the conductance to the infinite size limit gives additional credibility to the existence of a well-defined finite value of the conductance.

Turning now to the case of an odd number of sites L_s and repeating the procedure, the first difficulty appears: $L_s/2$ is not an integer number but an integer number of particles is needed to proceed. Fortunately, ground state energies for occupations $(L_s + 1)/2$ and $(L_s - 1)/2$ coincide and a linear combination of both degenerate states with equal weight $1/2$ produces a Green function describing perfect half-filling, that is, showing half a fermion per site. Using the same linear combination, exact Green functions are obtained for larger clusters that include additional non-interacting sites. Showing a behaviour quite dissimilar to the one found for the Hubbard model, conductance of any of these systems is exactly 1 when connected to leads via the Dyson equation. Therefore, conductances for spinless fermions interacting on an odd number of sites perfectly agree with the findings of [21] and [22], but the initially surprising results have an easy interpretation in view of the strong differences shown by the charge excitation spectra of both models. Figure 12 compares the exact density of states of 11-site clusters described either by the Hubbard model (upper panel) or by the spinless interacting model (lower panel). In both cases U is equal to 4 and a large imaginary part of $0.1t$ has been added to the excitation energy to show the δ-functions of the spectrum. Both are perfectly symmetric around 0 but while the Hubbard model shows a clear gap around the chemical potential, the spinless fermions model has a state at this energy. Moreover, even the

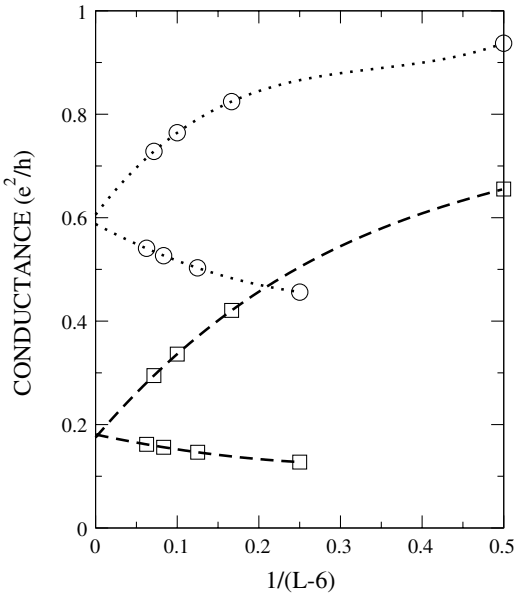

Figure 11. Scaling of the conductance of a connected chain of six sites in which spinless fermions interact according to the model of [21] and [22] as a function of the inverse of the number of salvage sites. Circles correspond to $U = 2$ and squares to $U = 4$. Polynomial fits take care of the even–odd dependence in the number of salvage sites at each side. Extrapolation gives conductances 0.60 ± 0.01 and 0.177 ± 0.003 for U equal to 2 and 4, respectively.

existence of a well-defined gap is not so clear for this model[10]. The zero energy excitation comes from the ambiguous number of particles inside the system, i.e. one more or one less particle comes into the system without an energy change. This particular excitation is the responsible—when coupled to the leads—of the perfect transmission at the chemical potential energy. On the other hand, the Hubbard model shows just a particle per site at half-filling and a typical cost for adding or removing one electron is $U/2$. As discussed above, although a dc current can traverse *small* Hubbard systems, their value systematically diminishes with the size of the system. In short, the particular behaviour of the spinless interacting system comes precisely from the substitution of the spin degeneration of the Hubbard model into systems of an odd number of sites by a charge degeneration that allows charge transport at zero energy cost, i.e. finite—actually perfect—dc conductance.

In this way, our whole numerical procedure has been indirectly checked through the comparison to the results obtained by the alternative numerical methods used to obtain conductances of spinless fermions through small interacting regions.

We would like to close this section by concluding that while our results support the accepted idea that the Hubbard model is an insulator at half-filling [20] they also give further insight into the transport of electrons through an interacting region. For example, the large value of the differential conductance for energies above the gap and its independence of the U value comes somewhat as a surprise. While small scattering is quite plausible for small values of U, one could expect large scattering for U values as large as twice the one-electron bandwidth.

[10] We are presently conducting a deeper study of the interacting spinless model aimed at answering the scaling behaviour of the model as a function of the number of *interacting* sites. Conductances at different filling ratios will also be investigated.

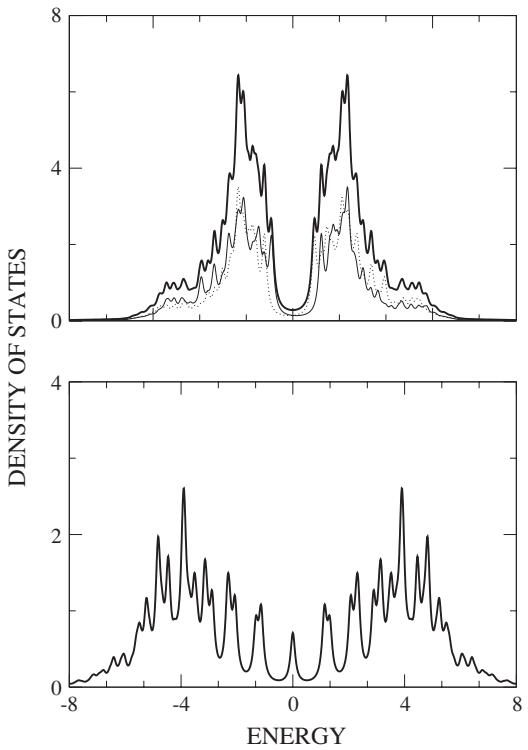

Figure 12. The density of states of an isolated Hubbard chain of 11 sites at half-filling (six electrons with spin up and five electrons with spin down) (upper panel) is compared with the same magnitude for the spinless fermionic model of [21] and [22] on a chain formed by 11 sites containing 5.5 fermions (lower panel). In both cases the value of U is 4 and the imaginary part added to the energy to show δ-functions is 0.1. Partial densities of up (continuous curve) and down (dotted curve) spin states are also given. Energies are given in terms of the hopping energy t while t^{-1} is used for the density of states.

3.3. Metallic system

Results for systems away from half-filling are presented in this section. In this situation, chemical potential is no longer $U/2$ as before and should be obtained for the finite cluster from ground state calculations with different numbers of particles. We define:

$$\mu_+ = E_0(N+1) - E_0(N)$$
$$\mu_- = E_0(N) - E_0(N-1),$$

where $E_0(N)$ represents the ground state energy corresponding to N particles and take the arithmetic mean of both:

$$\mu = (\mu_+ + \mu_-)/2.$$

The difference between both estimations is typically very small in this case (actually both should coincide away from half-filling in a closed Hubbard chain [19]). We always have $\mu < U/2$ when the number of particles is smaller than the number of sites. As said at the beginning of this section, this value of the chemical potential is also assumed for the connected system. Numerical results show that this assumption is internally consistent: the total number of electrons in the cluster and their spatial distribution hardly depend on the presence of the electrodes.

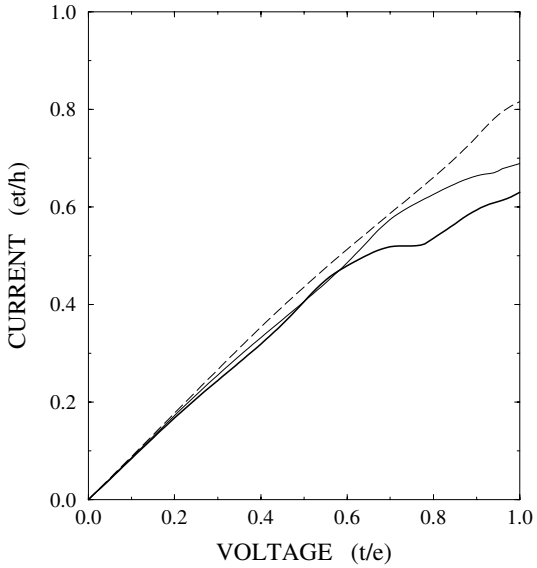

Figure 13. This figure illustrates the size independence of the metallic behaviour of the interacting system at one-quarter-filling. Current–voltage characteristics for lengths 8 (dashed curve), 12 (continuous curve), and 16 (thick curve) are compared.

The more important result in the metallic case is the length independence of the transport through the interacting part. This is shown by figure 13 for the current through 8, 12, and 16 Hubbard sites at one-quarter filling. For this comparison, a relatively large value $U = 4t$ of the interaction has been chosen. Differences between results corresponding to different lengths are probably measuring the typical precision of our approach. Additional numerical calculations not discussed in this paper help to show that all scattering occurs at the system contacts but not inside the interacting region. Let us proceed to the evaluation of the contact resistance and its dependence on U and the filling factor.

Figure 14 gives current–voltage curves for a chain of 12 interacting sites directly connected to metallic electrodes of constant (and large) density of states. The number of electrons within the cluster is always six while U increases from t to $8t$. Scattering at the contacts is always small regardless of the large values of U included in the figure. For example, the result for $U = 8t$ (twice the corresponding non-interacting bandwidth value) at $V = 0.5t/e$ can be explained by a transmission coefficient of about 0.87 at each interface. Actually, the approximate non-dependence on U is quite surprising.

Figure 15 gives current–voltage curves for the same system but the number of electrons in the cluster has been varied from 2 to 12 in steps of 2. In all cases a linear characteristic is obtained (better for small voltages) but the slope of the curve, i.e. the differential conductance, *strongly* depends on the filling factor (note that the slope of the IV curve is given by the current value at the smaller voltage value in a log–log graph). While differential conductance is close to its maximum value of one quantum for a large number of electrons (8 or 10), it is much smaller for small filling factors (two to six electrons in 12 sites). More precisely, the average conductance is 0.29 for two electrons, 0.51 for four electrons and 0.69 for six electrons (one-quarter filling factor). Although it is tempting to relate these values to experimentally measured values of conductances in clean quantum wires, we think that an improved geometrical model is necessary prior to a realistic comparison with experiments. (For example, the presence

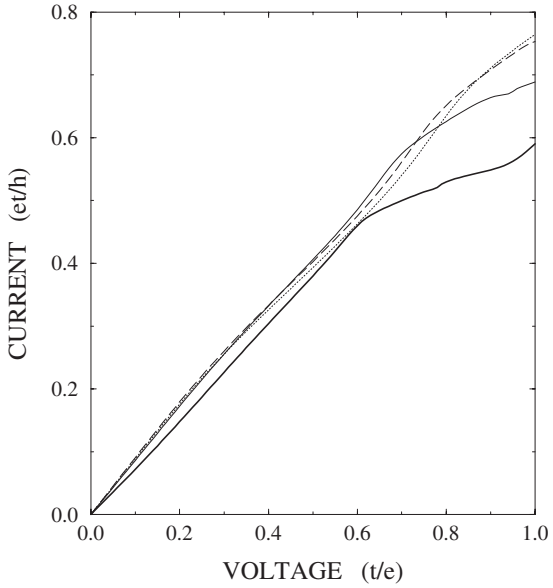

Figure 14. This figure illustrates the U dependence of the current–voltage curves in the metallic regime at one-quarter-filling. The correlation self-energy has been obtained for 12 sites and several U values. Results for $U/t = 1$, 2, 4, and 8 are given by dotted, long-dashed, thin, and thick curves, respectively.

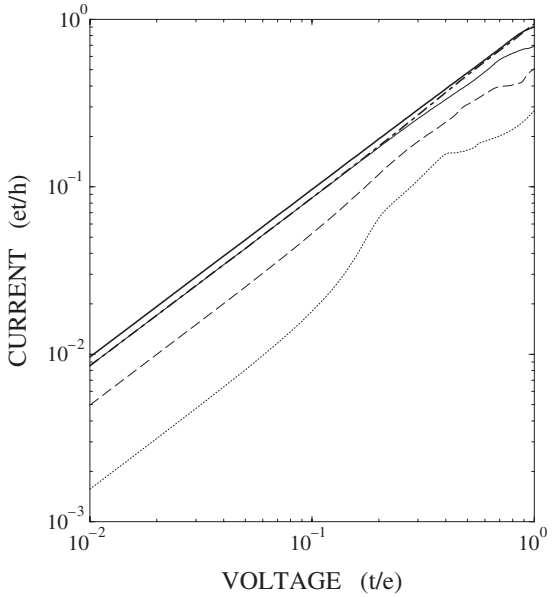

Figure 15. This figure illustrates the metallic behaviour of the interacting system at fillings others than half. Results correspond to 12 sites, $U = 4t$ and increasing numbers of electrons: $Q = 2$ (dotted curve), 4 (long-dashed curve), 6 (thin continuous line), 8 (dot–dashed curve), and 10 (thick continuous curve). Notice that the last three curves are very close to the maximum differential conductance (slope 1 in the units of the figure).

of several conducting channels that can be active as a function of the Fermi level should be accounted for.) Moreover, the consideration of long-range interactions among electrons can also change conclusions. In spite of these difficulties in approaching the real world, which will be explored in further work, it seems interesting that the major (maybe the unique) dependence of transport across an interacting system comes from the filling factor (from the chemical potential as observed from the electrodes) and not from the value of the interaction.

4. Summary

A general and computationally convenient method has been implemented for the evaluation of the current–voltage characteristics through interacting regions. The method has been checked by studying an isolated Anderson impurity in a linear chain. Two main results have been proved for extended Hubbard systems. First, the isolating behaviour at half-filling, including the possibility of activated transport for voltage values above the gap, has been shown. Our results confirm the physical picture obtained by studying the scaling of the Drude peak of half-filled Hubbard rings [20] but disagree in important details from previous studies in the same open geometry [4, 5]. For example, Kondo-like systems formed by an odd number of impurities show a resonance transmission that decays exponentially with the number of sites.

Second, good metallic behaviour has been obtained away from half-filling when the number of electrons is large enough. In this case, the interacting region allows ballistic electrons that are just scattered by the contacts between electrodes and the Hubbard part. The value of these contact resistances hardly depends on U but shows an important dependence on the filling factor or the chemical potential. Ballistic transport, that is, size-independent current for a given voltage, seems to exclude real scattering within the interacting sample and, therefore, exotic consequences of any interaction at $T = 0$. Although previously reported theoretical estimations of quasi-perfect transmittance [1–3] are partially confirmed in this one-dimensional metal–Luttinger liquid–metal setup just below half-filling, conductance is smaller at other filling factors. We guess that broader systems allowing several conductance channels are needed to correctly model the experimental phenomena observed in quantum wires.

Acknowledgments

E V Anda is acknowledged for fruitful discussions about the method. One of the authors (JAV) thanks R Aguado for helping in the development of the Anderson impurity section. This work has been partially supported by Buenos Aires University (grant UBACYT-EX210), Argentinian CONICET, Spanish Comisión Interministerial de Ciencia y Tecnología (grants PB96-0085 and MAT2002-04429), and Dirección General de Enseñanza Superior e Investigación y Ciencia (grant 1FD97-1358).

References

[1] Maslov D L and Stone M 1995 *Phys. Rev.* B **52** R5539
Maslov D L 1995 *Phys. Rev.* B **52** R14368
[2] Ponomarenko V V 1995 *Phys. Rev.* B **52** R8666
[3] Schulz H J 1995 *Proc. Les Houches Summer School* vol 61, ed E Akkermans, G Montambaux, J Pichard and J Zinn-Justin (Amsterdam: Elsevier) p 533 (*Preprint* cond-mat/9503150)
Safi I and Schulz H J 1995 *Phys. Rev.* B **52** R17040
[4] Oguri A 1999 *Phys. Rev.* B **59** 12240
Oguri A 2001 *Phys. Rev.* B **63** 115305
Oguri A 2001 *Phys. Rev.* B **64** 153305

[5] Oguri A 2001 *J. Phys. Soc. Japan* **70** 2666
[6] Odintsov A A, Tokura Y and Tarucha S 1997 *Phys. Rev.* B **56** R12729
Ponomarenko V V and Nagaosa N 1998 *Phys. Rev. Lett.* **81** 2304
Ponomarenko V V and Nagaosa N 1999 *Phys. Rev. Lett.* **83** 1822
[7] Caroli C, Combescot R, Nozieres P and Saint-James D 1971 *J. Phys. C: Solid State Phys.* **4** 916
[8] Meir Y and Wingreen N S 1992 *Phys. Rev. Lett.* **68** 2512
[9] Dagotto E 1994 *Rev. Mod. Phys.* **66** 763
[10] Keldysh L V 1964 *Zh. Eksp. Teor. Fiz.* **47** 1515
Keldysh L V 1965 *Sov. Phys.—JETP* **20** 1018 (Engl. Transl.)
[11] Landau L D and Lifshitz E M 1981 *Course of Theoretical Physics* vol 10 (Oxford: Pergamon)
[12] Mahan G D 1990 *Many-Particle Physics* 2nd edn (New York: Plenum)
[13] Yeyati A L, Martín-Rodero A and Flores F 1993 *Phys. Rev. Lett.* **71** 2991
[14] Davidovich M A, Anda E V, Iglesias J R and Chiappe G 1997 *Phys. Rev.* B **55** R7335
Ferrari V, Chiappe G, Anda E V and Davidovich M A 1999 *Phys. Rev. Lett.* **82** 5088
Büsser C A, Anda E V, Lima A L, Davidovich M A and Chiappe G 2000 *Phys. Rev.* B **62** 9907
[15] Robert S and Stevens K W H 1980 *J. Phys. C: Solid State Phys.* **13** 5941
Anda E V 1981 *J. Phys. C: Solid State Phys.* **14** L1037
da Rosa Simões A S, Iglesias J R, Rojo A and Alascio B R 1988 *J. Phys. C: Solid State Phys.* **21** 1941
[16] The role played by the electrochemical potential across a constriction has been addressed, for example, by
Pernas P L, Martín-Rodero A and Flores F 1990 *Phys. Rev.* B **41** 8553
Levy Yeyati A, Flores F and Anda E V 1993 *Phys. Rev.* B **47** 10543
[17] Ng T K and Lee P A 1988 *Phys. Rev. Lett.* **61** 1768
[18] Langreth D C 1966 *Phys. Rev.* **150** 516
[19] Lieb E H and Wu F Y 1968 *Phys. Rev. Lett.* **20** 1445
[20] Stafford C A, Millis A J and Shastry B S 1991 *Phys. Rev.* B **43** 13660
Fye R M, Martins M J, Scalapino D J, Wagner J and Hanke W 1991 *Phys. Rev.* B **44** 6909
[21] Molina R A, Weinmann D, Jalabert R A, Ingold G-L and Pichard J-L 2003 *Phys. Rev.* B **67** 235306
[22] Meden V and Schollwöck U 2003 *Phys. Rev.* B **67** 193303